ZO-1 and -2 Are Required for TRPV1-Modulated Paracellular Permeability

J. Li[1], X. Cong[2], Y. Zhang[2], R.L. Xiang[2], M. Mei[1], N.Y. Yang[3], Y.C. Su[2], S. Choi[4], K. Park[4], L.W. Zhang[5], L.L. Wu[2], and G.Y. Yu[1]

Abstract

The tight junction–based paracellular pathway plays an important role in saliva secretion. Zonula occludens (ZO) proteins are submembranous proteins of tight junction complex; however, their function in salivary epithelium is poorly understood. Here, we found that activation of transient receptor potential vanilloid subtype 1 (TRPV1) by capsaicin increased rat saliva secretion both in vivo and ex vivo. Meanwhile, TRPV1 activation enlarged the width of tight junctions between neighboring acinar cells, increased the paracellular flux of 4-kDa fluorescein isothiocyanate (FITC)-dextran in submandibular gland (SMG) tissues, and decreased transepithelial electric resistance (TER) in SMG-C6 cells. ZO-1, -2, and -3 were distributed principally to the apical lateral region of acinar cells in SMG tissues and continuously encircled the peripheries of SMG-C6 cells in the untreated condition. TRPV1 activation obviously diminished ZO-1 and -2 staining, but not ZO-3 or β-catenin, at the cell-cell contacts ex vivo and in vitro. Moreover, in untreated SMG-C6 cells, ZO-1 and -2 single or double knockdown by small interfering RNA (siRNA) increased the paracellular flux of 4-kDa FITC-dextran. In capsaicin-treated cells, ZO-1 and -2 single or double knockdown abolished, whereas their re-expression restored, the capsaicin-induced increase in paracellular permeability. Furthermore, TRPV1 activation increased RhoA activity, and inhibition of either RhoA or Rho kinase (ROCK) abolished the capsaicin-induced TER decrease as well as ZO-1 and -2 redistribution. These results indicate that ZO-1 and -2 play crucial roles in both basal salivary epithelial barrier function and TRPV1-modulated paracellular transport. RhoA-ROCK signaling pathway is responsible for TRPV1-modulated paracellular permeability as well as ZO-1 and -2 redistribution.

Keywords: zonula occludens, tight junction, capsaicin, transient receptor potential vanilloid subtype 1, salivary cells, salivation

Introduction

Tight junctions are localized at the most apical region of lateral membranes between neighboring cells, serving as a rate-limiting structure in regulating paracellular transport of fluid and solutes as well as a key constructor in maintaining the apico-basal epithelial polarity (Baker 2010). Tight junctions are integrated by interactions of transmembrane proteins, such as claudins and occludin, with submembranous proteins, like zonula occludens (ZO) proteins, including ZO-1, -2, and -3 (Shen et al. 2011). ZO proteins link tight junction proteins to the underlying actomyosin cytoskeleton and are speculated to be basic organizers and key modulators of tight junction structure and function (Bauer et al. 2010). In salivary glands, the tight junction–based paracellular pathway plays an important role in saliva secretion (Zhang et al. 2013). To date, ZO-1 has been found in mouse, rat, rabbit, and human salivary glands (Hashizume et al. 2004; Peppi and Ghabriel 2004; Maria et al. 2008; Cong et al. 2012). ZO-1 expression and distribution are altered in labial salivary glands from patients with Sjögren's syndrome as well as in hyposecretory rabbit submandibular gland (SMG) (Ewert et al. 2010; Cong et al. 2012), suggesting essential roles of ZO proteins in salivary epithelium. However, how ZO proteins regulate saliva secretion and the underlying mechanism are still poorly understood.

Transient receptor potential vanilloid subtype 1 (TRPV1) is a ligand-gated nonselective cation channel that can be activated by heat, acid, and capsaicin (Caterina et al. 1997). TRPV1 was originally found in the nervous system, following

[1]Department of Oral and Maxillofacial Surgery, Peking University School and Hospital of Stomatology, Beijing, China
[2]Department of Physiology and Pathophysiology, Peking University Health Science Center, Key Laboratory of Molecular Cardiovascular Sciences, Ministry of Education and Beijing Key Laboratory of Cardiovascular Receptors Research, Beijing, China
[3]Department of Pediatric Dentistry, Beijing Stomatological Hospital, Capital Medical University, Beijing, China
[4]Department of Physiology, School of Dentistry, Seoul National University, Seoul, South Korea
[5]Department of Oral Medicine, Peking University School and Hospital of Stomatology, Beijing, China

Corresponding Authors:
L.L. Wu, Department of Physiology and Pathophysiology, Peking University Health Science Center, Beijing 100191, China.
Email: pathophy@bjmu.edu.cn
G.Y. Yu, Department of Oral and Maxillofacial Surgery, Peking University School and Hospital of Stomatology, Beijing 100081, China.
Email: gyyu@263.net

discoveries in various nonneuronal tissues, including bladder epithelial cells and keratinocytes (Birder et al. 2001; Inoue et al. 2002). We have reported that TRPV1 is expressed in rat, rabbit, and human SMG, and TRPV1 activation by capsaicin increases saliva secretion partially via enhanced paracellular permeability (Zhang et al. 2006; Ding et al. 2010; Cong et al. 2013). However, the exact role of ZO proteins in TRPV1-mediated salivation and paracellular transport remains unknown.

Therefore, the present study was designed to explore the potential roles of ZO proteins in salivary epithelium and TRPV1-modulated paracellular permeability by using rat SMG and a rat SMG acinar cell line, SMG-C6.

Materials and Methods

Reagents and Antibodies

Zostrix cream with 0.075% capsaicin was obtained from Medicis Pharmaceutical (Scottsdale, AZ, USA). Capsaicin, capsazepine (CPZ), and 4-kDa fluorescein isothiocyanate (FITC)-dextran were purchased from Sigma-Aldrich Co. (St. Louis, MO, USA). C3 transferase, Rhotekin-RBD beads, and antibody to RhoA were from Cytoskeleton Inc. (Denver, CO, USA). Y-27632 was obtained from Tocris Bioscience (Bristol, UK). Antibodies to ZO-1, -2, and -3 and occludin were from Life Technologies (Carlsbad, CA, USA). The antibody to β-catenin was from Abmart (Shanghai, China). The antibody to β-actin was from Santa Cruz Biotechnology (Santa Cruz, CA, USA).

Measurement of Saliva Secretion

Capsaicin cream (0.075%, 0.2 g) was spread over the skin (2 × 2 cm^2) covering the SMG in healthy adult male Sprague-Dawley rats (250 to 300 g) at 9:00 to 11:00 am. Total saliva was collected every 5 min during 20 min before and after capsaicin cream application by putting a dry cotton swab into the mouth of the rat. The cotton swab was preweighed (Weight$_1$) and reweighed after collection (Weight$_2$). Saliva flow rate (mg/min) was calculated as (Weight$_2$ − Weight$_1$)/5 min. All experimental procedures were approved by the Ethics Committee of Animal Research, Peking University Health Science Centre, and complied with the Guide for the Care and Use of Laboratory Animals (NIH Publication No. 85-23, revised 1996). All animal research is reported in accordance with the ARRIVE guidelines (Kilkenny et al. 2010).

Perfusion of Isolated Rat SMG

The SMG was isolated and perfused through a polyethylene cannula placed in the external carotid artery under isoflurane anesthesia (Turner et al. 1996). The main excretory duct was cannulated for saliva collection. Krebs-Ringer-HEPES buffer (KRH, 37 °C, bubbled with 95% O$_2$ and 5% CO$_2$) was perfused to the glands for 30 min, and then different concentrations of capsaicin with or without CPZ were administered into the glands for 10 min. Saliva flow was measured as described by Schirmer's test (Fox et al. 1985).

Transmission Electron Microscopy

The SMG specimens were fixed and examined with a transmission electron microscope (Hitachi H-7000; Hitachi, Tokyo, Japan). The distances between neighboring tight junctions were measured with ImageJ software (National Institutes of Health, Bethesda, MD, USA).

Cell Culture and RT-PCR

SMG-C6 cells were cultured in Dulbecco's modified Eagle medium: Nutrient Mixture F-12 (DMEM/F-12) (1:1) as described previously (Quissell et al. 1997). Total RNA was extracted by Trizol (Invitrogen, Carlsbad, CA, USA) according to the manufacturer's instructions. The complementary DNA (cDNA) was prepared from 4 µg of total RNA with Moloney Murine Leukemia Virus (M-MLV) reverse-transcriptase (Promega, Madison, WI, USA). The primer sequences are shown in the Appendix Table. The products were separated by electrophoresis on a 1.5% agarose gel, and DNA bands were visualized by staining with ethidium bromide.

Western Blot Analysis

Proteins extracted from SMG tissues and cells were separated on 8% sodium dodecyl sulfate polyacrylamide gel electrophoresis (SDS-PAGE) and transferred to polyvinylidene difluoride membranes. The membranes were blocked with 5% nonfat milk, incubated with primary antibodies at 4 °C overnight, and probed with horseradish-peroxidase-conjugated secondary antibodies. The immunoreactive bands were visualized with enhanced chemiluminescence reagent (Pierce, Rockford, IL, USA).

Paracellular Tracer Flux Assay

The rat SMG was removed, cut into small pieces, and placed in a chamber (Costar, Corning, NY, USA) with KRH solution. Next, 4-kDa FITC-dextran (1 mg/mL) was added to KRH solution for 10 min, and then capsaicin was added to the solution. The pictures of acini were caught every 5 s under a confocal microscope (Leica TCS SP5; Leica, Wetzlar, Germany) as described previously (Segawa 1994). For the paracellular tracer flux assay in SMG-C6 cells, 4-kDa FITC-dextran was added to the medium in the basal compartment. After 3 h of incubation, a 200-µL aliquot of the medium was collected from the apical compartment, and the tracer flux was measured as the fluorescence intensity of FITC-dextran using a fluorometer (BioTek, Winooski, VT, USA) (Umeda et al. 2006).

Immunofluorescence Staining

The fixed SMG sections (7 µm thick) and cells were blocked in 1% bovine serum albumin for 30 min and then incubated with primary antibodies at 4 °C overnight, followed by incubation with secondary antibodies at 37 °C for 2 h. Nuclei were labeled with 4′,6-diamidino-2-phenylindole (DAPI). Fluorescence

images were captured using a confocal microscope. The fluorescent intensities were averaged by use of ImageJ software.

Preparation of Triton X-100 Insoluble and Soluble Fractions

Cells were lysed in ice-cold buffer (0.5% Triton X-100, 100 mmol/L NaCl, 10 mmol/L Tris-HCl, pH 7.4) at 4 °C for 20 min. Cell lysates were centrifuged at 13,000 × *g* for 30 min. The soluble supernatants were removed as the Triton X-100 soluble fractions. The remaining insoluble residues were resuspended as the Triton X-100 insoluble fractions (Kawedia et al. 2008).

Knockdown or Re-expression of ZO-1 and -2

SMG-C6 cells were cultured to 80% confluence and transfected with small interfering RNA (siRNA) using MegeTran 1.0 (Origene, Rockville, MD, USA). The potent rat siRNAs of ZO-1 5′-GAAGCUAUAUGAACGGUCUdTdT-3′ and ZO-2 5′-GCAAUAUAUGGCCCUAACAdTdT-3′, as well as the nonspecific control, were synthesized by Sigma-Aldrich Co. The cDNA clones of ZO-1 and -2 were from Addgene (Cambridge, MA, USA). Plasmid transfection was carried out and the cells were collected at least 24 h after transfection (Fanning et al. 2002; Oka et al. 2010).

Measurement of Transepithelial Electric Resistance

Confluent monolayers of SMG-C6 cells were grown in 24-well Transwell chambers (filter pore size: 0.4 μm; area: 0.33 cm^2; Costar, NY, USA) for 6 to 7 d. Transepithelial electric resistance (TER) was measured at 37 °C with an epithelial voltohmmeter (EVOM; World Precision Instruments, Sarasota, FL, USA). The background value of the filter (90 Ω) was subtracted, and all measurements were performed in triplicate.

RhoA Pull-Down Assay

RhoA pull-down assay was performed with Rhotekin-RBD beads. Tissues and cells were rapidly lysed in pull-down lysis buffer (50 mmol/L Tris, pH 7.5; 500 mmol/L NaCl; 10 mmol/L MgCl$_2$; and 2% IGEPAL, Sigma-Aldrich Co.) and centrifuged at 10,000 × *g* at 4 °C for 3 min. Equal amounts of the supernatant were incubated with Rhotekin-RBD beads at 4 °C with rotation for 1 h. The beads were washed and performed by Western blot analysis.

Statistical Analysis

Data are presented as mean ± SD. Statistical analyses were performed by 1-way or 2-way analysis of variance (ANOVA) and followed by Bonferroni's test using GraphPad Prism 5.0 (GraphPad Software, La Jolla, CA, USA). *P* < 0.05 was considered statistically significant.

Results

TRPV1 Activation Increases Saliva Secretion and Paracellular Permeability of Rat SMG

To detect the effect of capsaicin on saliva secretion, capsaicin cream was spread over the skin covering the SMG in rats. Capsaicin promoted saliva secretion during 20 min (Fig. 1A). The total amount of saliva within 20 min was significantly increased by application of capsaicin (Fig. 1B).

To explore the direct effect of capsaicin on the function and structure of SMG, we performed ex vivo perfusion into the isolated rat SMG. Capsaicin (10 and 20 μmol/L) significantly increased saliva secretion (Fig. 1C). Preperfusion with CPZ (10 μmol/L), a TRPV1 antagonist, abolished the capsaicin-increased saliva secretion. Tight junctions were located in the apical region of lateral membranes between neighboring acinar cells and formed a slightly dilated distance under transmitted electron microscope. The average width of tight junctions, used as an indicator of tight junction opening, was 10.87 ± 1.48 nm in KRH-perfused glands. Capsaicin enlarged the width of tight junctions, whereas CPZ preperfusion suppressed capsaicin-induced increase (Fig. 1D). The fluorescent intensity of 4-kDa FITC-dextran (1 mg/mL), a tracer frequently used for characterization of paracellular pathway, was increased in the acinar lumen after capsaicin (10 μmol/L) incubation. CPZ inhibited this response (Appendix Fig. 1). These results suggest that TRPV1-mediated salivation might involve an opening of the tight junction–based paracellular route.

TRPV1 Activation Induces the Redistribution of ZO-1 and -2

Expression of ZO-1, -2, and -3 messenger RNA (mRNA) and protein were detected in both rat SMG tissues and SMG-C6 cells (Appendix Fig. 2A, B). Immunofluorescence images revealed that ZO-1, -2, and -3 were localized principally to the apical lateral region in SMG tissues (Appendix Fig. 2C). In SMG-C6 cells, ZO-1, -2, and -3 characteristically formed the continuous staining encircling the cell peripheries and also dispersed in the cytoplasm.

In the capsaicin-perfused SMGs, ZO-1 and -2 stainings appeared discontinuous and were significantly decreased by 48.59% ± 6.86% and 53.43% ± 8.31%, respectively, in the apical lateral region (Fig. 2A), whereas ZO-3 was unaffected. The capsaicin-induced changes of ZO-1 and -2 were inhibited by CPZ pretreatment. Meanwhile, occludin staining was significantly reduced by 50.35% ± 4.04% at the cell-cell contacts after capsaicin perfusion, whereas the distribution of either claudin-3 or β-catenin was unaffected (Fig. 2B). Western blot analysis showed that the total amounts of ZO-1, -2, and -3, occludin, and β-catenin were not altered by capsaicin perfusion (Appendix Fig. 3).

In SMG-C6 cells, the double staining for ZO-1 and occludin from both horizontal (x-y) and vertical (x-z) planes revealed that ZO-1 and occludin were colocalized at the cell borders in untreated cells. Capsaicin (10 μmol/L) caused ZO-1 to partially disappear from cell-cell contacts at 5, 10, and 30 min, and it relocated to the cell borders at 60 min, in parallel with the alteration of occludin
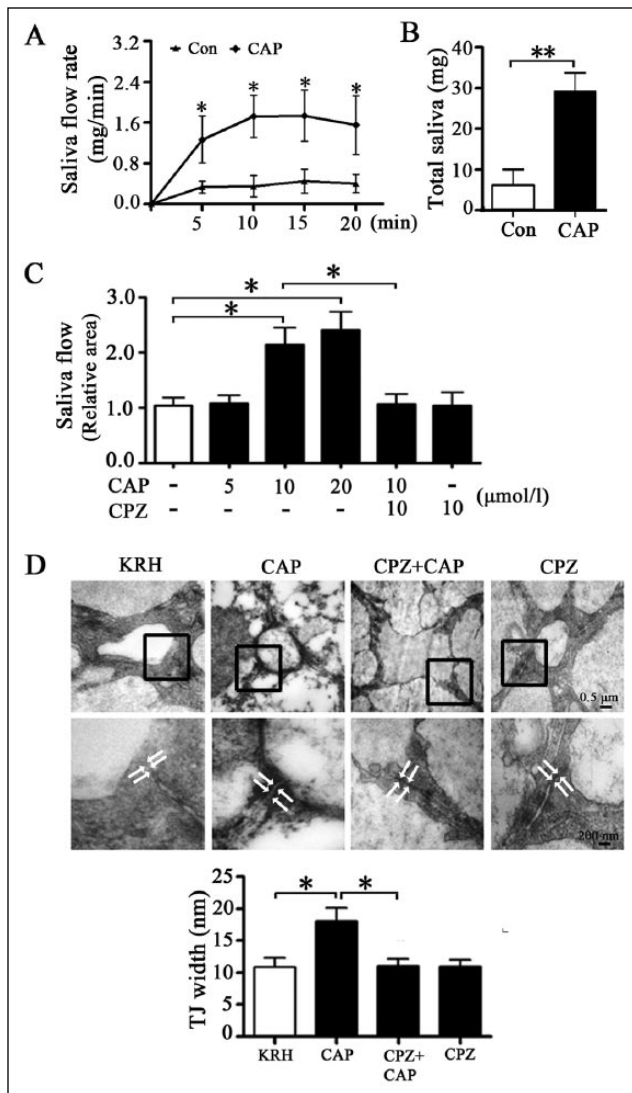
Figure 1. Activation of transient receptor potential vanilloid subtype 1 (TRPV1) increases saliva secretion and tight junction (TJ) width in rat submandibular gland (SMG). Capsaicin (CAP) cream (0.075%, 0.2 g) was spread over the skin (2 × 2 cm^2) covering the SMG. Total saliva was collected every 5 min during 20 min before and after CAP cream application by putting a dry cotton swab into the mouth of rats. The cotton swab was preweighed (Weight$_1$) and reweighed after collection (Weight$_2$). (**A**) Saliva flow rate [calculated as (Weight$_2$ − Weight$_1$)/5 min] and (**B**) total saliva volume were increased by CAP. Data are expressed as mean ± SD of 6 independent experiments. *$P < 0.05$ and **$P < 0.01$ vs. the control (Con). (**C**) Ex vivo perfusion was performed in the isolated rat SMG treated by different concentrations of CAP with or without capsazepine (CPZ, 10 μmol/L, 30 min) preperfusion. Saliva secretion was shown as the relative area (fold of control) of moisture on the filter paper. Data are expressed as mean ± SD of 4 independent experiments. *$P < 0.05$. (**D**) TJ ultrastructure was observed under transmitted electron microscope, and the distances between neighboring TJs (shown as the width of apical TJs) from 4 sections of 10 randomly selected fields each in 4 groups were measured. Data are expressed as mean ± SD of 4 independent experiments. *$P < 0.05$. Scale bars: 0.5 μm and 200 nm. KRH, Krebs-Ringer-HEPES buffer.

(Fig. 3A). Similar changes were observed for ZO-2 (Fig. 3B). The distribution of ZO-3 was unaffected by capsaicin (Fig. 3C, D).
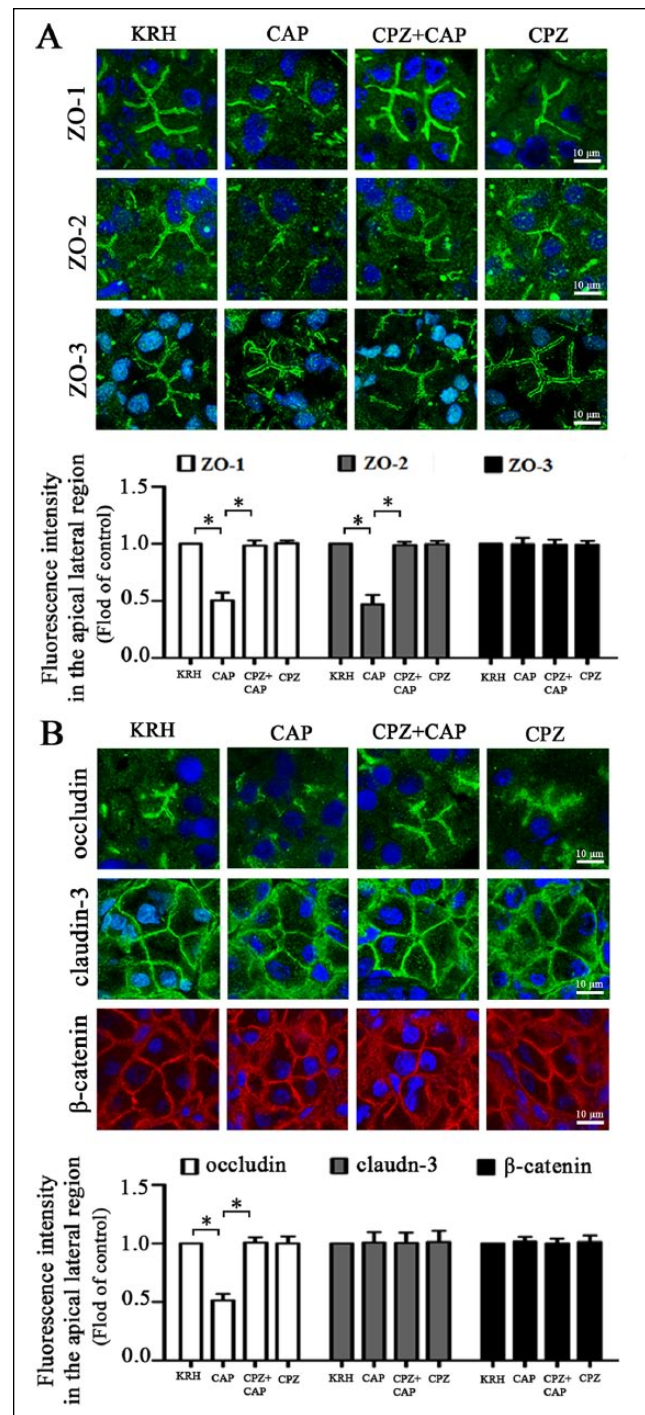

Figure 2. Activation of transient receptor potential vanilloid subtype 1 (TRPV1) induces redistribution of zonula occludens (ZO)-1 and -2, but not ZO-3, in rat submandibular gland (SMG). (**A, B**) Immunofluorescence staining of ZO-1 (A, upper panels), ZO-2 (A, middle panels), and ZO-3 (A, lower panels) as well as distributions of occludin (B, upper panels), claudin-3 (B, middle panels), and β-catenin (B, lower panels) induced by capsaicin (CAP, 10 μmol/L, 10 min) with or without capsazepine (CPZ) (10 μmol/L, 30 min) pretreatment in rat SMG along with quantification analysis for fluorescence intensities of these proteins in the apical lateral region. Data expressed as mean ± SD of 4 independent experiments. *$P < 0.05$. Scale bars: 50 μm and 10 μm. KRH, Krebs-Ringer-HEPES buffer.
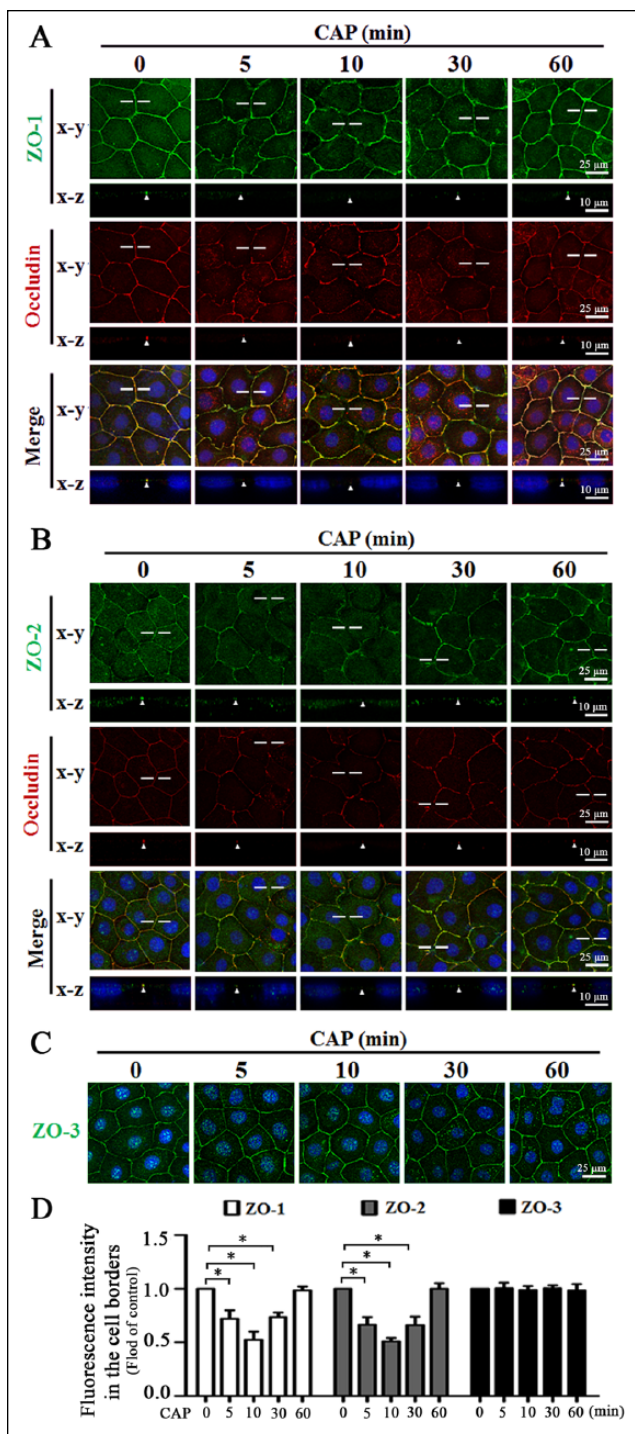
Figure 3. Capsaicin (CAP) induces redistribution of zonula occludens (ZO)-1 and -2, but not ZO-3, in SMG-C6 cells. (**A, B**) Distributions of double immunofluorescence staining of ZO-1 (A, upper panels) with occludin (A, middle panels) as well as ZO-2 (B, upper panels) with occludin (B, middle panels) induced by CAP (10 µmol/L) for the indicated time points at x-y and x-z planes. Scale bars: 25 µm and 10 µm. (**C**) Immunofluorescence staining of ZO-3 induced by CAP for the indicated time points at x-y planes. Scale bars: 25 µm. (**D**) Quantification analysis for fluorescent intensities of ZO-1, -2, and -3 at the cell-cell contacts. Data expressed as mean ± SD of 4 independent experiments. *$P < 0.05$.

Furthermore, the double staining confirmed that TRPV1 activation selectively induced redistribution of ZO-1 and -2 but not β-catenin (Appendix Fig. 4). Western blot analysis showed that the total protein levels of ZO-1, -2, and -3 and β-catenin were not changed by capsaicin treatment within 60 min (Appendix Fig. 5A). However, capsaicin induced ZO-1 and -2 decreases in the Triton X-100 insoluble fractions, concomitant with increases in the soluble fractions at 5, 10, and 30 min, and then recovered to basal levels at 60 min (Appendix Fig. 5B, C), suggesting a rapid and reversible translocation of ZO-1 and -2 from the tight junction complex into the cytoplasm. The levels of ZO-3 and β-catenin in either insoluble or soluble fractions were unaffected.

Knockdown of ZO-1 and -2 Alters Paracellular Permeability in SMG-C6 Cells

Next, we examined roles of ZO-1 and -2 in determining the paracellular permeability of SMG-C6. In ZO-1 and -2 single or double knockdown cells, the levels of ZO-3, occludin, and β-catenin were not affected (Fig. 4A–C). There were no significant differences in the basal TER values among ZO-1, ZO-2, ZO-1/-2 knockdown, and scrambled cells (Fig. 4D–F). Capsaicin caused a prominent drop in TER values from 5 to 60 min in scrambled cells, whereas the responses were significantly inhibited in the ZO-1 and -2 single or double knockdown cells. Moreover, the decreased TER reappeared in these corresponding reexpressed (rescue) cells (Fig. 4G–I). Paracellular flux assay revealed that the flux of 4-kDa FITC-dextran was significantly increased in ZO-1, ZO-2, and ZO-1/-2 knockdown cells compared with the scrambled cells, whereas the flux was restored to basal levels in the rescue cells (Fig. 4J–L). Capsaicin significantly increased the tracer flux in the scrambled cells but had no further effect in the knockdown cells. The responses reappeared in the rescue cells.

RhoA-ROCK Signaling Pathway Is Involved in TRPV1-Modulated Paracellular Permeability and Redistribution of ZO-1 and -2

We next explored the possible intracellular signaling pathway. Capsaicin significantly increased RhoA activity in both perfused SMG and cultured SMG-C6 cells (Fig. 5A, B). Preincubation with CPZ blocked the capsaicin-induced increase in RhoA activity ex vivo and in vitro (Fig. 5A, C). Furthermore, pretreatment with either RhoA inhibitor C3 transferase or Rho kinase (ROCK) inhibitor Y27632 suppressed the capsaicin-induced TER decrease (Fig. 5D, E) as well as the translocation of ZO-1 and -2 from Triton X-100 insoluble fractions into soluble fractions (Fig. 5F, G). Immunofluorescence staining further confirmed that the capsaicin-induced ZO-1 and -2 redistribution was suppressed by inhibition of RhoA-ROCK signaling pathway (Fig. 5H).

Discussion

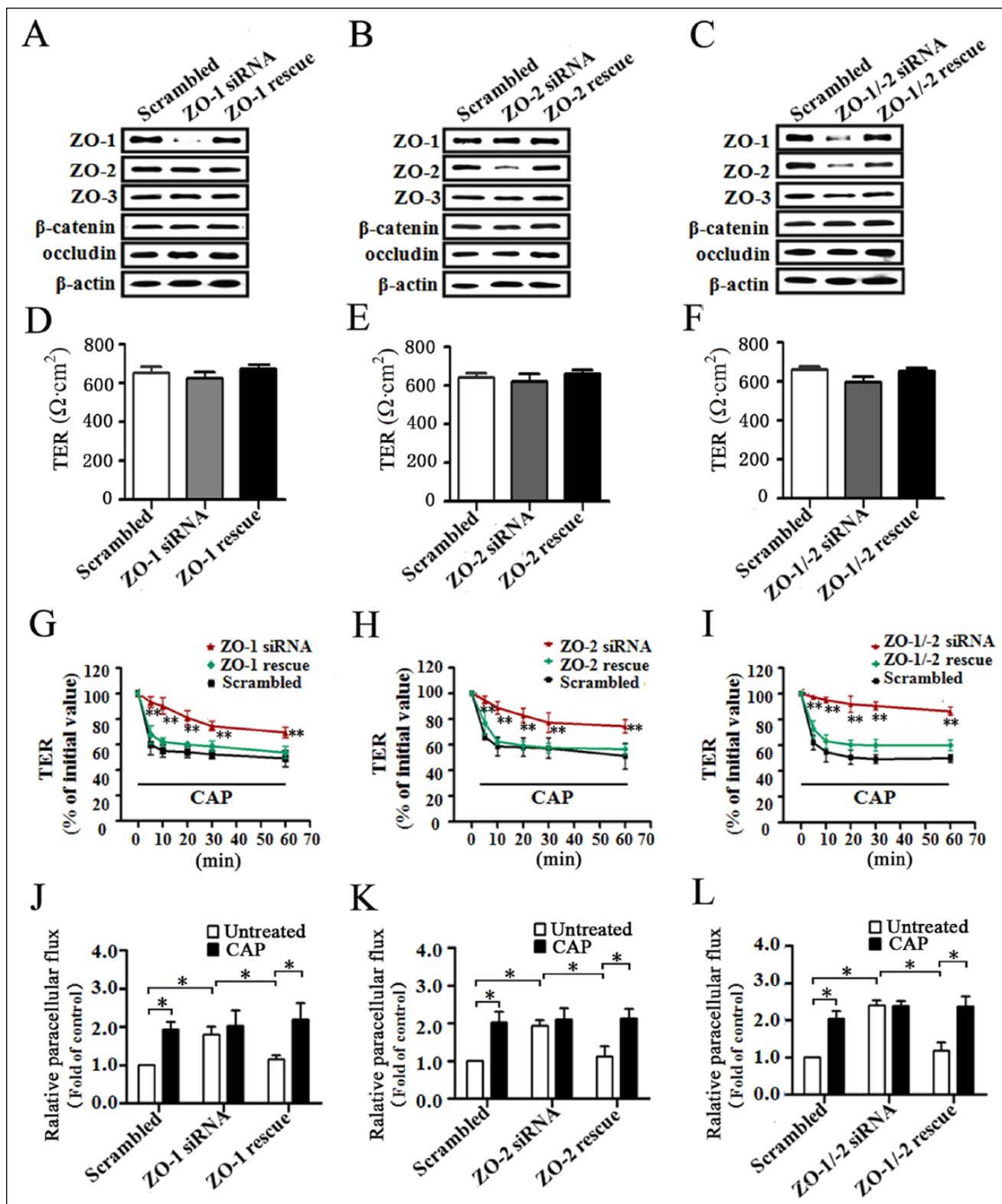In the present study, we demonstrate that ZO-1 and -2 are essential components in tight junction barrier function in rat

Figure 4. Zonula occludens (ZO)-1 and -2 are required for the capsaicin (CAP)-induced increase in paracellular permeability. (**A–C**) Western blot analysis of the expression of ZO-1, -2, and -3, β-catenin, and occludin in SMG-C6 cells transfected with ZO-1 and/or ZO-2 small interfering RNA (siRNA) as well as in the rescue cells by transfection of ZO-1 and/or ZO-2 complementary DNA (cDNA) into the knockdown cells. (**D–F**) Transepithelial electric resistance (TER) values of ZO-1 and/or ZO-2 knockdown and rescue cells in the untreated condition. Data expressed as mean ± SD of 4 independent experiments. (**G–I**) TER values of ZO-1 and/or ZO-2 knockdown and rescue cells treated with CAP (10 µmol/L). Data expressed as mean ± SD of 4 independent experiments. **$P < 0.01$ vs. the scrambled cells. (**J–L**) The paracellular flux assay for 4-kDa fluorescein isothiocyanate (FITC)-dextran in ZO-1 and/or ZO-2 knockdown and rescue cells with or without capsaicin treatment. Data expressed as mean ± SD of 4 independent experiments. *$P < 0.05$.
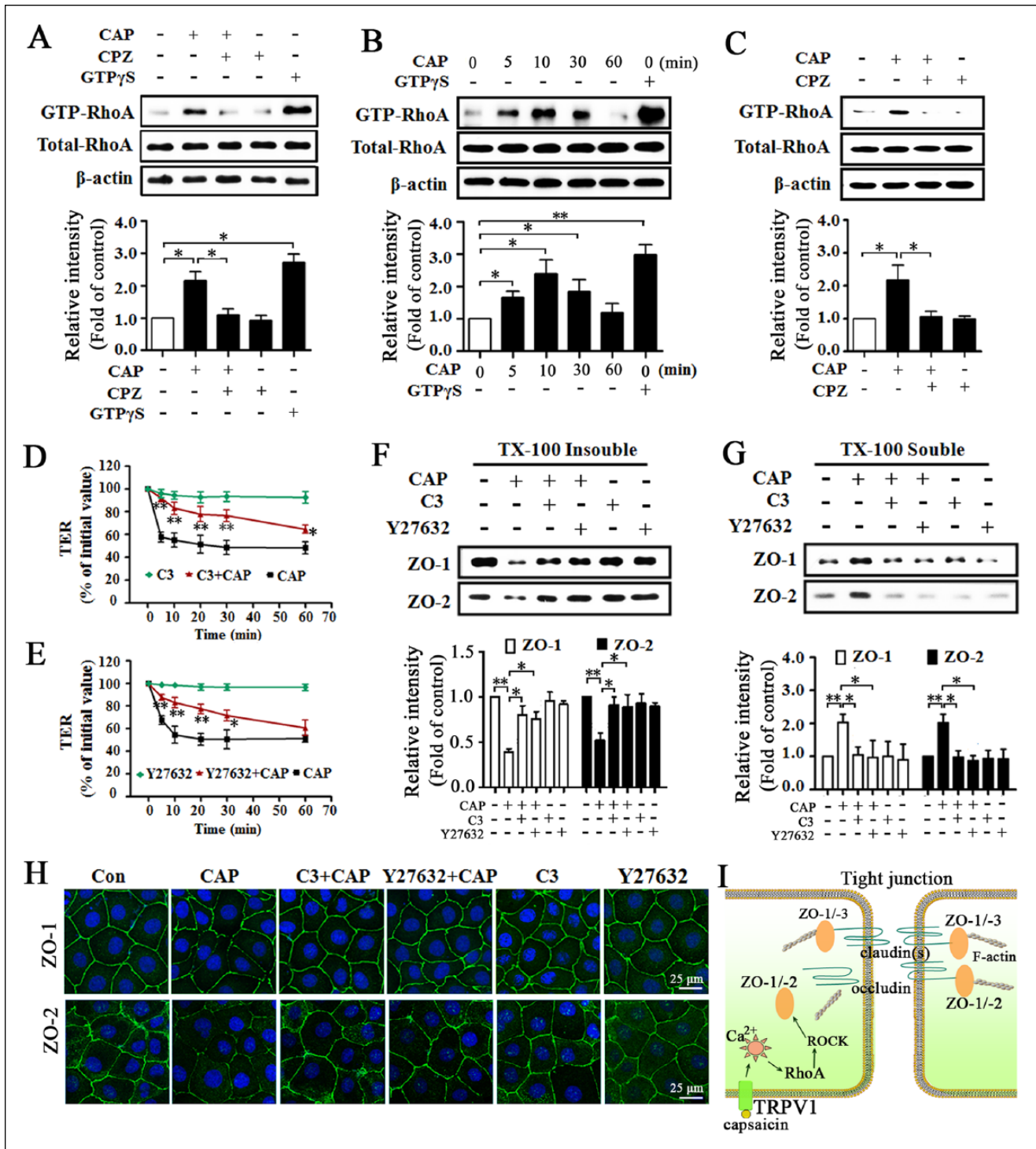
Figure 5. The signaling pathway for RhoA and Rho kinase (ROCK) is involved in transient receptor potential vanilloid subtype 1 (TRPV1)–modulated paracellular permeability as well as redistribution of zonula occludens (ZO)-1 and -2. (**A–C**) RhoA pull-down assay in rat submandibular gland (SMG) (A) and SMG-C6 cells (B, C) treated by capsaicin (CAP, 10 μmol/L) with or without capsazepine (CPZ, 10 μmol/L, 30 min) pretreatment. GTPγS (guanosine 5′-O-[gamma-thio]triphosphate) was used as a positive control. Data expressed as mean ± SD of 4 independent experiments. *$P < 0.05$ and **$P < 0.01$. (**D, E**) Transepithelial electric resistance (TER) values of SMG-C6 cells treated by CAP with or without either C3 transferase (C3, 1 μg/mL, 120 min) or Y27632 (10 μmol/L, 30 min) pretreatment. Data expressed as mean ± SD of 4 independent experiments. *$P < 0.05$ and **$P < 0.01$ vs. CAP-treated cells. (**F, G**) Western blot analysis of ZO-1 and -2 expressions induced by CAP with or without either C3 transferase or Y27632 pretreatment in Triton X-100 (TX-100) insoluble and soluble fractions of SMG-C6 cells. Data expressed as mean ± SD of 4 independent experiments. *$P < 0.05$ and **$P < 0.01$. (**H**) Immunofluorescence staining of ZO-1 and -2 distribution induced by CAP with or without either C3 transferase or Y27632 pretreatment. Each image is representative of 4 independent experiments. Scale bars: 25 μm. (**I**) Schematic illustrations showing the possible signaling pathway of TRPV1-modulated ZO proteins distribution in rat SMG cells. Con, control.

submandibular epithelial cells. The redistribution of ZO-1 and -2 from tight junctions into the cytoplasm plays a critical role in TRPV1-induced increases in paracellular permeability ex vivo and in vitro. Furthermore, the RhoA-ROCK signaling pathway is responsible for TRPV1-modulated ZO-1 and -2 redistribution. These results reveal an important role of ZO proteins in both basal and TRPV1-modulated tight junction properties and characterize a novel mechanism of TRPV1-modulated paracellular transport in SMG.

ZO proteins play vital roles in tight junction structure and function. Targeted deletion of either ZO-1 or -2 in mice leads to embryonic lethality, whereas ZO-3 deficiency does not show any abnormity (Adachi et al. 2006; Katsuno et al. 2008; Xu et al. 2008). Knockdown of either ZO-1 or -2, but not ZO-3, in cultured epithelial cells leads to delayed formation of tight junctions and an increase in paracellular flux, whereas exogenous expression of either of the two proteins alleviates the mutant phenotype (Adachi et al. 2006; Umeda et al. 2006; Van Itallie et al. 2009). Thus, ZO-1 and -2 have been considered as critical determinants of barrier structure and pivotal regulators of barrier function (Fanning and Anderson 2009). However, few data are available on the function and significance of ZO proteins in salivary epithelium. Here, we characterized that ZO-1, -2, and -3 were mainly localized to the apical lateral region and scattered in the cytoplasm in submandibular epithelial cells. As reported previously, TER reflects that ions pass through the claudin-based charge-selective pores (~4 Å in radius) with instantaneous (typically in seconds) high permeability, whereas paracellular flux assay indicates that large solutes (>4 Å in radius) pass through the so-called "leaky pathway" with lower permeability that is measured over much longer intervals (typically >2 h) (Srinivasan et al. 2015). Here, we showed that the TER values were not different, whereas the flux of 4-kDa FITC-dextran significantly increased in the ZO-1, ZO-2, or ZO-1/-2 knockdown cells compared with the scrambled control cells in untreated condition, and these changes were reversed by reexpression of ZO-1 and/or ZO-2. These results suggest that ZO-1 and -2 are essential elements to maintain the barrier function and that they might exert a specific effect on the permeability of large solutes without an obvious influence on the ionic permeability in normal salivary epithelium. A similar phenomenon has been observed in Eph4 and MDCK cells (Umeda et al. 2006; Fanning et al. 2012).

Next we explored the role of ZO proteins in TRPV1-modulated tight junction barrier function. Activation of TRPV1 markedly increased paracellular permeability of SMG as characterized by increased flux of 4-kDa FITC-dextran and decreased TER. Knockdown of ZO-1 and -2 alone or in combination partially abolished the capsaicin-induced increase in paracellular permeability, whereas their rescue restored this paracellular permeability. These results further indicate a critical requirement of ZO-1 and -2 in TRPV1-modulated tight junction barrier function. Furthermore, the increased paracellular permeability was accompanied by an increased saliva secretion, which suggests that the TRPV1-promoted saliva secretion is mediated, at least in part, by paracellular transport through ZO-1 and -2. As previously reported, application of capsaicin to the apex of the tongue or to the palatal mucosa induces salivation through the parasympathetic cholinergic pathway (Dunér-Engström et al. 1986). We found

that capsaicin promotes saliva secretion in vivo and ex vivo in rat, rabbits, and healthy volunteers, indicating that TRPV1 activation can directly stimulate saliva secretion in SMG (Zhang et al. 2006; Cong et al. 2012; Ding et al. 2010).

Numerous studies have shown that changes in the subcellular distribution of ZO proteins in response to various stimuli are often in association with altered tight junction structure and barrier function (Nusrat et al. 2000). For example, acute lung injury induces ZO-1 redistribution accompanied by disruption of barrier integrity in pulmonary epithelium (Jacob and Gaver 2012). Renal ischemia-reperfusion injury causes ZO-1 relocalization followed by disrupted barrier function in rat kidney tissues (Lee et al. 2011). Accordingly, ZO-1 has been recognized as a marker for the integrity of tight junctions (Hurd et al. 2003; Xu et al. 2011). Here, we found that TRPV1 activation selectively induced ZO-1 and -2 redistribution, but not ZO-3 or β-catenin, in both SMG tissues and SMG-C6 cells, suggesting that ZO-1 and -2 are involved in TRPV1-modulated tight junction barrier function by altering their subcellular distribution.

We further explored the signaling pathway linking TRPV1 to ZO proteins. The RhoA-ROCK signaling pathway is considered to play important roles in regulating ZO proteins (González-Mariscal et al. 2008). In Eph4 cells, RhoA activator ARHGEF11 mediates ZO-1-dependent junction assembly and barrier formation (Itoh et al. 2012). In intestinal epithelium, RhoA activity is required for the increased paracellular permeability and relocation of ZO-1 in response to leptin stimulation (Le Dréan et al. 2014). Here, we provide additional evidence that the RhoA-ROCK signaling pathway is involved in modulating tight junction properties of salivary epithelium. TRPV1 activation increased RhoA activity ex vivo and in vitro. Inhibition of the RhoA-ROCK signaling pathway abolished the capsaicin-induced TER decrease as well as redistribution of ZO-1 and -2, indicating that TRPV1-modulated changes in tight junction barrier function and structure are mediated by the RhoA-ROCK signaling pathway.

In summary, we provide the first evidence that ZO-1 and -2 are crucial elements in maintaining tight junction barrier integrity and are key targets in TRPV1-modulated paracellular transport in rat submandibular epithelium. As well, we found that the RhoA-ROCK signaling pathway mediates the TRPV1-induced redistribution of ZO-1 and -2 as well as the increase in paracellular permeability (schematic illustration shown in Fig. 5I). These findings highlight the functional significance of ZO-1 and -2 in salivary epithelial cells and enrich our understanding of the mechanism involved in TRPV1-modulated saliva secretion.

Author Contributions

J. Li, contributed to data acquisition, analysis and interpretation, drafted the manuscript; X. Cong, contributed to data interpretation and analysis, critically revised the manuscript; Y. Zhang, contributed to data interpretation, critically revised the manuscript; R.L. Xiang, contributed to data analysis, critically revised the manuscript; M. Mei, N.Y. Yang, Y.C. Su, S. Choi, L.W. Zhang, contributed to data acquisition, critically revised the manuscript; K. Park, contributed to conception, critically revised the manuscript; L.L. Wu, G.Y. Yu, contributed to conception and design, critically revised the manuscript. All authors have given final approval and agree to be accountable for all aspects of the work.

Acknowledgments

References

Adachi M, Inoko A, Hata M, Furuse K, Umeda K, Itoh M, Tsukita S. 2006. Normal establishment of epithelial tight junctions in mice and cultured cells lacking expression of ZO-3, a tight-junction MAGUK protein. Mol Cell Biol. 26(23):9003–9015.

Baker OJ. 2010. Tight junctions in salivary epithelium. J Biomed Biotechnol. 2010:278948.

Bauer H, Zweimueller-Mayer J, Steinbacher P, Lametschwandtner A, Bauer HC. 2010. The dual role of zonula occludens (ZO) proteins. J Biomed Biotechnol. 2010:402593.

Birder LA, Kanai AJ, de Groat WC, Kiss S, Nealen ML, Burke NE, Dineley KE, Watkins S, Reynolds IJ, Caterina MJ. 2001. Vanilloid receptor expression suggests a sensory role for urinary bladder epithelial cells. Proc Natl Acad Sci USA. 98(23):13396–13401.

Caterina MJ, Schumacher MA, Tominaga M, Rosen TA, Levine JD, Julius D. 1997. The capsaicin receptor: a heat-activated ion channel in the pain pathway. Nature. 389(6653):816–824.

Cong X, Zhang Y, Shi L, Yang NY, Ding C, Li J, Ding QW, Su YC, Xiang RL, Wu LL, et al. 2012. Activation of transient receptor potential vanilloid subtype 1 increases expression and permeability of tight junction in normal and hyposecretory submandibular gland. Lab Invest. 92(5):753–768.

Cong X, Zhang Y, Yang NY, Li J, Ding C, Ding QW, Su YC, Mei M, Guo XH, Wu LL, et al. 2013. Occludin is required for TRPV1-modulated paracellular permeability in the submandibular gland. J Cell Sci. 126(Pt 5):1109–1121.

Ding QW, Zhang Y, Wang Y, Wang YN, Zhang L, Ding C, Wu LL, Yu GY. 2010. Functional vanilloid receptor-1 in human submandibular glands. J Dent Res. 89(7):711–716.

Dunér-Engström M, Fredholm BB, Larsson O, Lundberg JM, Saria A. 1986. Autonomic mechanisms underlying capsaicin induced oral sensations and salivation in man. J Physiol. 373:87–96.

Ewert P, Aguilera S, Alliende C, Kwon YJ, Albornoz A, Molina C, Urzúa U, Quest AF, Olea N, Pérez P, et al. 2010. Disruption of tight junction structure in salivary glands from Sjogren's syndrome patients is linked to proinflammatory cytokine exposure. Arthritis Rheum. 62(5):1280–1289.

Fanning AS, Anderson JM. 2009. Zonula occludens-1 and -2 are cytosolic scaffolds that regulate the assembly of cellular junctions. Ann N Y Acad Sci. 1165:113–120.

Fanning AS, Ma TY, Anderson JM. 2002. Isolation and functional characterization of the actin binding region in the tight junction protein ZO-1. FASEB J. 16(13):1835–1837.

Fanning AS, Van Itallie CM, Anderson JM. 2012. Zonula occludens-1 and -2 regulate apical cell structure and the zonula adherens cytoskeleton in polarized epithelia. Mol Biol Cell. 23(4):577–590.

Fox PC, van der Ven PF, Sonies BC, Weiffenbach JM, Baum BJ. 1985. Xerostomia: evaluation of a symptom with increasing significance. J Am Dent Assoc. 110(4):519–525.

González-Mariscal L, Tapia R, Chamorro D. 2008. Crosstalk of tight junction components with signaling pathways. Biochim Biophys Acta. 1778(3):729–756.

Hashizume A, Ueno T, Furuse M, Tsukita S, Nakanishi Y, Hieda Y. 2004. Expression patterns of claudin family of tight junction membrane proteins in developing mouse submandibular gland. Dev Dyn. 231(2):425–431.

Hurd TW, Gao L, Roh MH, Macara IG, Margolis B. 2003. Direct interaction of two polarity complexes implicated in epithelial tight junction assembly. Nat Cell Biol. 5(2):137–142.

Inoue K, Koizumi S, Fuziwara S, Denda S, Inoue K, Denda M. 2002. Functional vanilloid receptors in cultured normal human epidermal keratinocytes. Biochem Biophys Res Commun. 291(1):124–129.

Itoh M, Tsukita S, Yamazaki Y, Sugimoto H. 2012. Rho GTP exchange factor ARHGEF11 regulates the integrity of epithelial junctions by connecting ZO-1 and RhoA-myosin II signaling. Proc Natl Acad Sci USA. 109(25):9905–9910.

Jacob AM, Gaver DP 3rd. 2012. Atelectrauma disrupts pulmonary epithelial barrier integrity and alters the distribution of tight junction proteins ZO-1 and claudin 4. J Appl Physiol. 113(9):1377–1387.

Katsuno T, Umeda K, Matsui T, Hata M, Tamura A, Itoh M, Takeuchi K, Fujimori T, Nabeshima Y, Noda T, et al. 2008. Deficiency of zonula occludens-1 causes embryonic lethal phenotype associated with defected yolk sac angiogenesis and apoptosis of embryonic cells. Mol Biol Cell. 19(6):2465–2475.

Kawedia JD, Jiang M, Kulkarni A, Waechter HE, Matlin KS, Pauletti GM, Menon AG. 2008. The protein kinase A pathway contributes to Hg^{2+}-induced alterations in phosphorylation and subcellular distribution of occludin associated with increased tight junction permeability of salivary epithelial cell monolayers. J Pharmacol Exp Ther. 326(3):829–837.

Kilkenny C1, Browne W, Cuthill IC, Emerson M, Altman DG; NC3Rs Reporting Guidelines Working Group. 2010. Animal research: reporting in vivo experiments: the ARRIVE guidelines. Br J Pharmacol. 160(7):1577–1579.

Le Dréan G, Haure-Mirande V, Ferrier L, Bonnet C, Hulin P, de Coppet P, Segain JP. 2014. Visceral adipose tissue and leptin increase colonic epithelial tight junction permeability via a RhoA-ROCK-dependent pathway. FASEB J. 28(3):1059–1070.

Lee SY, Shin JA, Kwon HM, Weiner ID, Han KH. 2011. Renal ischemia-reperfusion injury causes intercalated cell-specific disruption of occludin in the collecting duct. Histochem Cell Biol. 136(6):637–647.

Maria OM, Kim JW, Gerstenhaber JA, Baum BJ, Tran SD. 2008. Distribution of tight junction proteins in adult human salivary glands. J Histochem Cytochem. 56(12):1093–1098.

Nusrat A, Parkos CA, Verkade P, Foley CS, Liang TW, Innis-Whitehouse W, Eastburn KK, Madara JL. 2000. Tight junctions are membrane microdomains. J Cell Sci. 113(Pt 10):1771–1781.

Oka T, Remue E, Meerschaert K, Vanloo B, Boucherie C, Gfeller D, Bader GD, Sidhu SS, Vandekerckhove J, Gettemans J, et al. 2010. Functional complexes between YAP2 and ZO-2 are PDZ domain-dependent, and regulate YAP2 nuclear localization and signalling. Biochem J. 432(3):461–472.

Peppi M, Ghabriel MN. 2004. Tissue-specific expression of the tight junction proteins claudins and occludin in the rat salivary glands. J Anat. 205(4):257–266.

Quissell DO, Barzen KA, Gruenert DC, Redman RS, Camden JM, Turner JT. 1997. Development and characterization of SV40 immortalized rat submandibular acinar cell lines. In Vitro Cell Dev Biol Anim. 33(3):164–173.

Segawa A. 1994. Tight junction permeability in living cells: dynamic changes directly visualized by confocal laser microscopy. J Electron Microsc. 43(5):290–298.

Shen L, Weber CR, Raleigh DR, Yu D, Turner JR. 2011. Tight junction pore and leak pathways: a dynamic duo. Annu Rev Physiol. 73:283–309.

Srinivasan B, Kolli AR, Esch MB, Abaci HE, Shuler ML, Hickman JJ. 2015. TEER measurement techniques for in vitro barrier model systems. J Lab Autom. 20(2):107–126.

Turner JT, Sullivan DM, Rovira I, Camden JM. 1996. A regulatory role in mammalian salivary glands for 5-hydroxytryptamine receptors coupled to increased cyclic AMP production. J Dent Res. 75(3):935–941.

Umeda K, Ikenouchi J, Katahira-Tayama S, Furuse K, Sasaki H, Nakayama M, Matsui T, Tsukita S, Furuse M, Tsukita S. 2006. ZO-1 and ZO-2 independently determine where claudins are polymerized in tight-junction strand formation. Cell. 126(4):741–754.

Van Itallie CM, Fanning AS, Bridges A, Anderson JM. 2009. ZO-1 stabilizes the tight junction solute barrier through coupling to the perijunctional cytoskeleton. Mol Biol Cell. 20(17):3930–3940.

Xu J, Kausalya PJ, Phua DC, Ali SM, Hossain Z, Hunziker W. 2008. Early embryonic lethality of mice lacking ZO-2, but not ZO-3, reveals critical and nonredundant roles for individual zonula occludens proteins in mammalian development. Mol Cell Biol. 28(5):1669–1678.

Xu LF, Xu C, Mao ZQ, Teng X, Ma L, Sun M. 2011. Disruption of the F-actin cytoskeleton and monola7yer barrier integrity induced by PAF and the protective effect of ITF on intestinal epithelium. Arch Pharm Res. 34(2):245–251.

Zhang GH, Wu LL, Yu GY. 2013. Tight junctions and paracellular fluid and ion transport in salivary glands. Chin J Dent Res. 16(1):13–46.

Zhang Y, Xiang B, Li YM, Wang Y, Wang X, Wang YN, Wu LL, Yu GY. 2006. Expression and characteristics of vanilloid receptor 1 in the rabbit submandibular gland. Biochem Biophys Res Commun. 345(1):467–473.